Simultaneous investigation of shear modulus and torsional resonance of solid ^{4}He

Jaeho Shin,[1] Jaewon Choi,[1] Keiya Shirahama,[2] and Eunseong Kim[1,*]
[1]*Center for Supersolid and Quantum Matter Research, KAIST, Daejeon, Republic of Korea*
[2]*Department of Physics, Keio University, Yokohama, Japan*
(Received 14 March 2016; revised manuscript received 17 May 2016; published 20 June 2016)

We investigate the origin of a resonant period drop of a torsional oscillator (TO) containing solid ^{4}He by inspecting its relation to a change in elastic modulus. To understand this relationship directly, we measure both phenomena simultaneously using a TO with a pair of concentric piezoelectric transducers inserted in its annulus. We confirm experimentally that both anomalies are directly related. Although the temperature, ^{3}He concentration, and frequency dependence are essentially the same, a marked discrepancy in the drive amplitude dependence is observed. We find that this discrepancy originates from the anisotropic response of polycrystalline solid ^{4}He connected with low-angle grain boundaries by studying the shear modulus parallel to and perpendicular to the driving direction.

DOI: 10.1103/PhysRevB.93.214512

I. INTRODUCTION

The change in the shear modulus μ and the dissipation Q^{-1} of solid ^{4}He at low temperature [1–9] have been understood thoroughly by the Granato-Lucke (GL) model [10–12]. According to this model, in a dislocation network, dislocations glide under applied stress, which leads to an additional strain field. This strain decreases the μ of a solid from its intrinsic value. However, the slip motion can be effectively damped by binding of dislocation segments with impurities at low temperatures. The pinning of dislocations is regulated by the finite binding energy, E_b, between dislocations and impurities in a solid, such that the pinning can be promoted only at sufficiently low temperatures. These weakly bound impurities on the dislocations are detached as a result of increasing temperature and/or external stress, which can be described by the Debye relaxation process and characterized by a relaxation time τ and an activation energy E_b [4,8,9]. Solid ^{4}He is a golden testbed for the GL model because the only impurities in solid ^{4}He are an extremely low concentration of ^{3}He atoms. The properties of dislocation in solid ^{4}He, such as the average network length, dislocation density, and length distribution, have been extensively studied by Balibar and coworkers [5–9].

Another interesting observation of solid ^{4}He is that the resonant period of a torsional oscillator (TO) containing solid ^{4}He decreases below 0.2 K [13–25]. This was initially interpreted as a result of the reduction of the rotational inertia of solid ^{4}He, and considered as the appearance of a putative supersolid phase. Nevertheless, both the μ and TO response exhibited fundamentally identical dependences on the temperature, driving amplitude, frequency, and amount of ^{3}He impurities [1,25,26]. To investigate the underlying relationships between them, Kim *et al.* [25] measured the shear modulus change ($\Delta\mu$) and the resonant period drop (Δprd) simultaneously by inserting a pair of flat piezoelectric transducers (PZT) into the center of a TO. Even though a similar temperature dependence was observed, the drive amplitude responses were different. When a large ac voltage was applied to a driving transducer, $\Delta\mu$ of solid ^{4}He at the center channel was fully suppressed, but Δprd of the TO was not significantly affected. Similarly, the influence of a TO drive on the μ measurements was also minor; μ did not deviate from the unaffected value until the TO drive suppressed all of the nonclassical responses of the TO. To explain this discrepancy in the drive amplitude dependence, the authors suggested that there were ultimately different microscopic origins between the two phenomena. However, one could question the validity of this interpretation since the measurements were performed in different locations in the TO cell; hence, the discrepancy could be attributed to the different solid samples.

II. SIMULTANEOUS EXPERIMENTS

Here, we present a new TO design in order to overcome the above-mentioned problems by utilizing a pair of concentric PZT inserted into the annular channel of a TO cell, as shown in Fig. 1. This allows us to measure the TO response and $\Delta\mu$ originating from the same solid sample. The design of a TO capable of simultaneous measurements is not straightforward because it is necessary to selectively eliminate the influence of the complex geometry of a TO, and to directly associate the change in μ to the response of a TO. Recent studies [27–33] have indicated that the inappropriate design of a TO would amplify the elastic effect of solid ^{4}He. The analysis of the response in a nonideal TO is not simple and is often misinterpreted. The discrepancies found in previous simultaneous measurements [25] can also be attributed to the complicated structure of the TO. Accordingly, it is crucial that the response of a TO should not be associated with the change in the μ in a complicated way, so that one can conclude clearly whether or not both phenomena are directly connected.

We constructed a TO without any internal structure in order to eliminate a potential source of complexity in the analysis of the TO response. The Maris effect [30] in the current TO design is suppressed since the TO has the same topological structure as a torus constructed with a thick Be-Cu plate connected to a torsion rod by stainless steel screws. On the other hand, the glue effect [31–33] is caused by relative motion between the components of a TO cell, which can be enhanced further when a TO is not rigidly constructed. Solid ^{4}He in the narrow annular channel of the current TO is expected to exhibit the glue effect

*Corresponding author: eunseong@kaist.edu

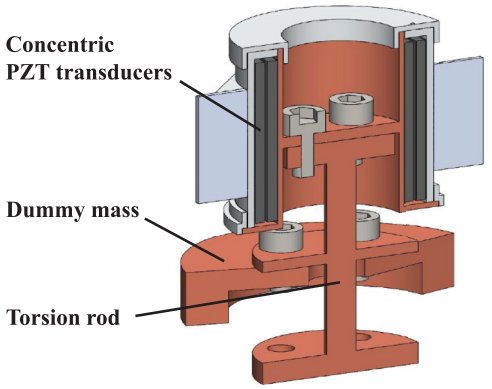

FIG. 1. Double-frequency torsional oscillator containing a pair of concentric piezoelectric transducers.

by consolidating the motion of the inner and outer TO walls at low temperatures. Since solid ^{4}He is sandwiched between the inner and outer PZTs, it is possible to measure the $\Delta\mu$, which is directly coupled to the TO response. For small changes in the elastic modulus, a quantitative change in the resonance period can be simulated using a finite element method (FEM) simulation. FEM simulations enable us to obtain the optimum design of a TO in order to maximize the simple coupling of the change in μ to the TO response.

Besides, to confirm the origin of the TO response experimentally, we constructed a double-frequency TO so that the elastic effect can be examined via frequency analysis [33,34]. The resonance frequency of the lower mode (f_-) is 548 Hz and that of the higher mode (f_+) is 1280 Hz. The mechanical Q values are 1.99×10^6 for the f_- mode and 4.08×10^5 for the f_+ mode. We grew solid ^{4}He using the conventional blocked capillary method, which is known to produce polycrystalline samples consisting of numerous randomly oriented micrometer-sized grains. The pressure of the sample cannot be measured directly due to the blockage in the capillary during the growth and, thus, was obtained by measuring the freezing temperatures. It is ranging from 45 to 65 bars and no obvious pressure dependence was found during this simultaneous measurement. We studied solid ^{4}He grown with various ^{3}He impurity concentrations, x_3, of 0.6, 5, 10, 20, 75, 150, and 300 ppb. The ratios of the period reduction, Δprd, to the solid mass loading, ΔP, Δprd/ΔP, were approximately 0.5% for the f_- mode and approximately 3% for the f_+ mode at low temperature. The disagreement in Δprd/ΔP between two modes is inconsistent with the genuine superfluid response of a TO. The ratios were normalized with the low-temperature saturation values to elucidate the temperature dependence as shown in Fig. 2(a).

Figure 2 shows the changes in μ and the TO responses measured under various conditions as a function of temperature. With isotopically pure ^{4}He, the intermediate crossover temperature, T_i, where μ or Δprd/ΔP drops of the low-temperature saturated value was found to be approximately 27 mK in both measurements. We found T_i increased with increasing x_3 and reached approximately 60 mK with commercially available ^{4}He with a nominal x_3 of 300 ppb. This demonstrates that the temperature and x_3 dependences in both measurements are clearly identical. When the TO and PZT were driven at a higher

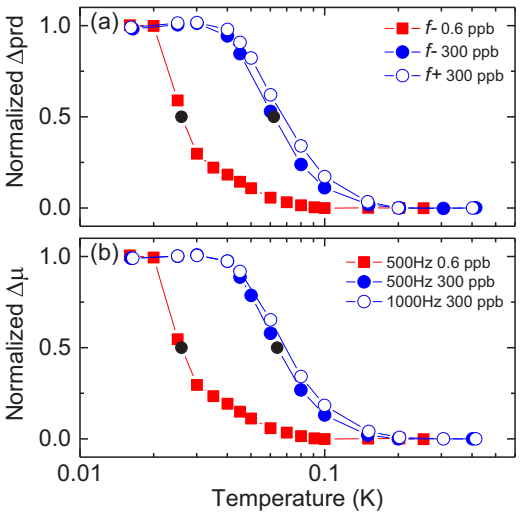

FIG. 2. Temperature, x_3, and frequency dependence of (a) resonance period of TO and (b) shear modulus. Square (red) and circle (blue) symbols indicate the temperature behaviors for 0.6- and 300-ppb samples. Closed and open symbols represent the measurement frequency and black dots indicate T_i.

frequency, T_i was shifted to a higher temperature, as expected in the framework of dislocation pinning by ^{3}He impurities.

The most striking observation is that the drive dependence for both measurements shows an apparent discrepancy. In order to study the drive dependence, the μ and resonant period are measured, respectively, as a function of temperature with various frequencies and driving amplitudes. Then, $\Delta\mu$ and Δprd at 18 mK were extracted. These data at various measurement frequencies were normalized to highlight the drive dependence more clearly and plotted as a function of applied stress, as shown in Fig. 3. Because the elasticity of

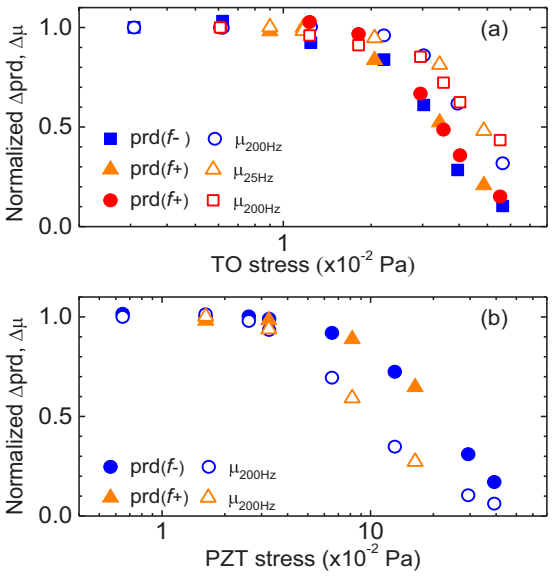

FIG. 3. Normalized Δprd (open symbols) and $\Delta\mu$ (closed symbols) are shown as a function of applied stress. The influence of (a) TO stress and (b) shear stress on resonance period and μ measurements. Different colors indicate different frequencies.

solid ^{4}He can be altered by two independent driving sources, the PZT drive and the TO drive, two sets of data were collected individually to investigate the effect of drive dependence. Both the PZT and TO responses to the TO driving stress were monitored while maintaining the PZT driving amplitude to a minimum in order to prevent its undesired additional influence. The apparent discrepancy stands out when the drive dependences of the two phenomena are plotted together in Fig. 3(a). The TO stress value was calculated from the oscillation amplitude. Although both show a qualitatively similar response, the quantitative dependence on the driving amplitude was not identical. The μ measurement was not changed until the magnitude of the driving stress increased to 0.02 Pa, where the TO response exhibited strong suppression by 15% of the entire Δprd. The TO responses for two separate frequencies follow the same drive dependence, whereas the μ traces a distinctly different path with the dependence shifted to the higher drive side. Similarly, the PZT-induced stress dependence is measured by holding the TO amplitude at a minimum. The stress caused by the PZT was converted from the driving voltage. The normalized drive dependences of both responses to PZT-induced stress are shown in Fig. 3(b). In contrast to the previous set of TO stress measurements, increasing the PZT drive causes a suppression of μ first without changing the TO response while the current simultaneous measurements were performed on the same solid sample. The threshold stress to induce suppression for the μ measurement is approximately 0.1 Pa, and that for the TO measurement is approximately 0.03 Pa.

Accordingly, it is very tempting to attribute the discrepancy in the simultaneous measurements to the different microscopic origins of the two phenomena, suggesting that the TO anomaly is possibly due to the putative supersolid phase. However, a number of recent studies [27,28,32,33] have strongly disproved the supersolid explanation. These TO studies demonstrate clearly that the TO anomaly does not exist in the ideal TO [27] or that the supersolid fraction should be less than 4 ppm [32], indicating that the large TO anomaly was mainly due to the elastic effect of solid ^{4}He.

We were able to determine experimentally whether or not the period reduction could be entirely explained by the change in elastic modulus of solid ^{4}He. Figure 4(a) shows the period change of the f_+ mode, $\Delta\text{prd}(f_+)$, as a function of that of the f_- mode, $\Delta\text{prd}(f_-)$, in solid samples containing various ^{3}He. When $\Delta\mu$ of solid ^{4}He is the underlying mechanism for both anomalies, $\Delta\text{prd}(f_+)$ increases faster than that expected in the ideal mass decoupling of solid ^{4}He. This is because the change in period due to the elastic effect is proportional to the f^2. Accordingly, the slope of the elastic effect can be steeper by a factor of $(f_+/f_-)^2$. Figure 4(a) shows various evolutions of $\Delta\text{prd}(f_+)$ versus $\Delta\text{prd}(f_-)$ expected with different scenarios. The steeper gray solid line exhibits the evolution due to the elastic stiffening of helium obtained from the FEM simulation. On the other hand, the blue dashed line shows the expectation from the mass decoupling superfluid and the red dotted line is the elastic modulus change scenario that is steeper by the factor of $(f_+/f_-)^2$ to the superfluid one. These are analytic expectations from the f_+ and f_- mode of TO [34]. The experimental data with various x_3 show excellent agreement with the elastic modulus change scenario.

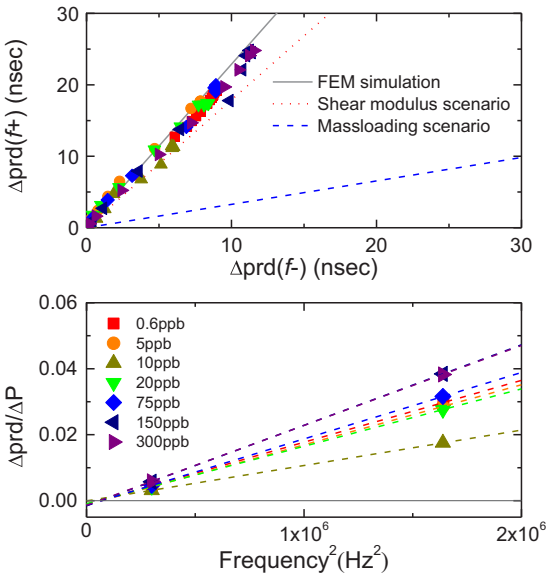

FIG. 4. (a) Ratio of Δprd for f_+ mode to f_- mode with different x_3. (b) Result of frequency analysis for frequency-independent contribution.

Furthermore, we could extract the frequency-independent superfluid contribution by subtracting f^2-dependent terms which can be attributed to the $\Delta\mu$ from the double-frequency TO results [34]. Nearly zero mass decoupling is observed, as shown in Fig. 4(b), which is consistent with the implications of the ratio analysis and the same analysis performed in rigid double torus TO measurements [33]. Based on both analyses, we concluded that Δprd of the TO anomaly is intrinsically originated from the elastic effect of solid ^{4}He.

We noticed that there were two key differences in the driving methods of the two measurements that might lead to the discrepancy in the drive dependence: the spatial profile of the strain along the driving direction and the orientation of the stress. First, the applied strain is uniform in the annulus when solid ^{4}He is driven by a PZT [1], while the strain due to torsional oscillation is expected to be parabolic with the maximum at the center of the annular channel and the minima at the confining annular walls [35]. Despite the generic differences in the spatial profile, the same drive dependence in both measurements should have been observed. It is because of the fact that the time average of $\Delta\mu$ is not susceptible to the spatial profile, but mainly to the average stress applied to the solid ^{4}He. Second, the directions of stress produced by both measurements were perpendicular to each other. The TO drive produced strain along the direction of torsional oscillation, whereas the concentric PZT induced strain and stress along the cylindrical axis of the TO cell, perpendicular to the TO drive. Nevertheless, these differences are expected to be irrelevant because solid samples grown by the blocked capillary method were considered to be isotropic.

The elastic modulus of a single crystal of solid ^{4}He [5] can be quantitatively determined using the Bond matrix, which converts the elastic tensor, C, in a crystal coordinate system to the elastic tensor, C', in a transducer coordinate system. The C of a hexagonal close-packed crystal consists of five independent elastic components (c_{11}, c_{12}, c_{13}, c_{33} and

c_{44}) [36–38]. A comprehensive study of an oriented single crystal of solid ^{4}He instructed that the elastic anomaly of solid ^{4}He is ascribed to the motion of dislocation on the Basal plane and can be described quantitatively by only the reduction in c_{44} [5]. All 36 components in the elastic tensor C' are generally nonzero and represent various values, depending on the relative angles between the crystal and transducer. Thus, the μ measurements of a single crystal of solid ^{4}He reveal strong anisotropy. On the other hand, a polycrystalline solid ^{4}He is composed of a sufficiently large number of grains with random orientations. The elastic tensor of a polycrystalline solid is isotropic and can be expressed by two independent values: Young's modulus E and Poisson's ratio ν. Thus, the discrepancies in the drive dependence would not be expected if the measurements were performed on a proper polycrystal. Although the blocked capillary grown samples are considered to be a proper polycrystal, we attempted to confirm the validity of this hypothesis by measuring the stress that developed both perpendicular and parallel to the driving direction.

III. A STACKED PZT CELL STUDY

We constructed a new PZT-only cell in order to clarify the above issue. The schematic illustration of the PZT transducers only cell is shown in Fig. 5. Two planar transducers (10 mm in height, 10 mm in width, and 2 mm in thickness) on the detection side were stacked in such a way that the polarizing directions were perpendicular to each other. This enabled us to measure the μ parallel to the direction of the drive and in the perpendicular direction [39]. On the driving side, two PZTs were stacked in the same way, so as to apply strain in both the perpendicular and parallel directions.

Figure 6 shows the set of anisotropic responses for both PZTs during the measurements performed on four different samples that include two blocked capillary grown samples (S01, S02), an extensively annealed sample (S03), and a quench cooled sample (S04). Remarkably, the responses in both orientations clearly reveal the different drive dependences, despite the temperature dependences for each orientation being very similar. In addition, the anisotropic drive dependence remains essentially the same, regardless of the dramatically different sample preparation procedures. The

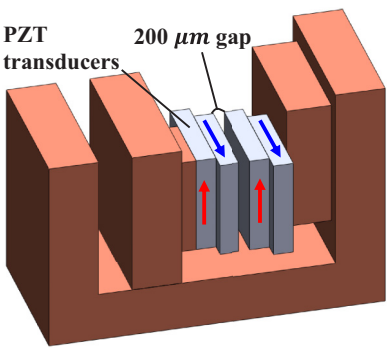

FIG. 5. Perpendicularly stacked shear PZT cell. The arrows indicate the polarizing direction of PZTs.

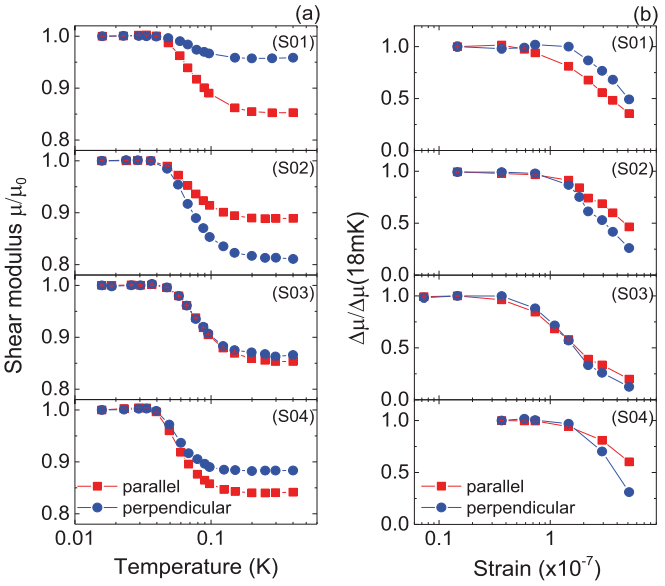

FIG. 6. (a) Temperature and (b) driving amplitude dependence of μ for different solid samples at 18 mK. Square symbols (red) indicate a parallel direction measurement. Circle symbols (blue) indicate a perpendicular direction measurement.

drive and temperature response of the extensively annealed sample (S03) seems isotropic but the quantitative discrepancy is apparent. The particularly different "isotropic" response is likely due to the certain orientation of the sample S03 with respect to both transducers. For instance, if the c axis of hcp helium, assuming a large single crystal, is almost parallel to the driving PZT then similar response can be observed in both measurements. Besides, additional extensive annealing of S03 was carried out to investigate the unusual response, which led to the vastly anisotropic response. The result is consistent with a few annealing experiments that show no clear evidence of the "good" annealing effect; improving the crystal quality by reducing the number of grains.

These anisotropic behaviors are not expected in a polycrystalline sample, as discussed earlier, revealing that the solid ^{4}He between the transducers is composed of a few highly oriented crystals or a sufficiently small number of domains connected with a certain preferential orientation. While a small grain size of 10 μm or less was reported in a mass injected cell [40], thermal conductivity [41,42] and x-ray-diffraction measurements [43] reported the grain sizes of approximately 0.1 mm or larger.

IV. CONCLUSION

In summary, the unbinding of ^{3}He impurities from dislocation lines is a fundamental mechanism to decrease the shear modulus of solid ^{4}He at high temperature and/or high stress. The temperature and ^{3}He dependence in both TO and shear modulus measurements can be understood straightforwardly in this framework. The reported anisotropy in the orientation-dependent drive response, on the other hand, has been a long-standing question and is often used as counter-evidence against a nonsupersolid interpretation. Our sophisticated design of

simultaneous TO and shear modulus measurements with the capability of frequency analysis enables us to understand the underlying connection deeply. The anisotropy arises from solid ^{4}He grown with a certain preferential orientation, indicating that both anomalies are originated from the same mechanism of a change in elastic property of solid ^{4}He, rather than the emergence of supersolidity.

ACKNOWLEDGMENTS

This work was supported by a National Research Foundation of Korea grant funded by the Korean government Ministry of Science, ICT and Future Planning (MSIP) (Grant No. 2007-0054-848) and by a Grant-in-Aid for Scientific Research (Grant No. 21224010) from the Japan Society for the Promotion of Science.

[1] J. Day and J. Beamish, Nature (London) **450**, 853 (2007).
[2] J. Day, O. Syshchenko, and J. Beamish, Phys. Rev. B **79**, 214524 (2009).
[3] J. Day, O. Syshchenko, and J. Beamish, Phys. Rev. Lett. **104**, 075302 (2010).
[4] O. Syshchenko, J. Day, and J. Beamish, Phys. Rev. Lett. **104**, 195301 (2010).
[5] A. Haziot, X. Rojas, A. D. Fefferman, J. R. Beamish, and S. Balibar, Phys. Rev. Lett. **110**, 035301 (2013).
[6] A. Haziot, A. D. Fefferman, J. R. Beamish, and S. Balibar, Phys. Rev. B **87**, 060509 (2013).
[7] A. Haziot, A. D. Fefferman, F. Souris, J. R. Beamish, H. J. Maris, and S. Balibar, Phys. Rev. B **88**, 014106 (2013).
[8] A. D. Fefferman, F. Souris, A. Haziot, J. R. Beamish, and S. Balibar, Phys. Rev. B **89**, 014105 (2014).
[9] F. Souris, A. D. Fefferman, H. J. Maris, V. Dauvois, P. Jean-Baptiste, J. R. Beamish, and S. Balibar, Phys. Rev. B **90**, 180103 (2014).
[10] A. Granato and K. Lücke, J. Appl. Phys. **27**, 583 (1956).
[11] L. J. Teutonico, A. Granato, and K. Lücke, J. Appl. Phys. **35**, 220 (1964).
[12] K. Lücke, A. Granato, and L. Teutonico, J. Appl. Phys. **39**, 5181 (1968).
[13] E. Kim and M. H. W. Chan, Science **305**, 1941 (2004).
[14] E. Kim and M. H. W. Chan, Nature (London) **427**, 225 (2004).
[15] Ann Sophie C. Rittner and J. D. Reppy, Phys. Rev. Lett. **97**, 165301 (2006).
[16] Ann Sophie C. Rittner and J. D. Reppy, Phys. Rev. Lett. **98**, 175302 (2007).
[17] Ann Sophie C. Rittner and J. D. Reppy, Phys. Rev. Lett. **101**, 155301 (2008).
[18] Y. Aoki, J. C. Graves, and H. Kojima, Phys. Rev. Lett. **99**, 015301 (2007).
[19] A. C. Clark, J. T. West, and M. H. W. Chan, Phys. Rev. Lett. **99**, 135302 (2007).
[20] A. Penzev, Y. Yasuta, and M. Kubota, Phys. Rev. Lett. **101**, 065301 (2008).
[21] J. T. West, X. Lin, Z. G. Cheng, and M. H. W. Chan, Phys. Rev. Lett. **102**, 185302 (2009).
[22] B. Hunt, E. Pratt, V. Gadagkar, M. Yamashita, A. Balatsky, and J. Davis, Science **324**, 632 (2009).
[23] H. Choi, S. Kwon, D. Kim, and E. Kim, Nat. Phys. **6**, 424 (2010).
[24] H. Choi, D. Takahashi, K. Kono, and E. Kim, Science **330**, 1512 (2010).
[25] D. Y. Kim, H. Choi, W. Choi, S. Kwon, E. Kim, and H. C. Kim, Phys. Rev. B **83**, 052503 (2011).
[26] E. Kim, J. S. Xia, J. T. West, X. Lin, A. C. Clark, and M. H. W. Chan, Phys. Rev. Lett. **100**, 065301 (2008).
[27] D. Y. Kim and M. H. W. Chan, Phys. Rev. Lett. **109**, 155301 (2012).
[28] D. Y. Kim, J. T. West, T. A. Engstrom, N. Mulders, and M. H. W. Chan, Phys. Rev. B **85**, 024533 (2012).
[29] J. R. Beamish, A. D. Fefferman, A. Haziot, X. Rojas, and S. Balibar, Phys. Rev. B **85**, 180501 (2012).
[30] H. J. Maris, Phys. Rev. B **86**, 020502 (2012).
[31] J. D. Reppy, X. Mi, A. Justin, and E. J. Mueller, J. Low Temp. Phys. **168**, 175 (2012).
[32] D. Y. Kim and M. H. W. Chan, Phys. Rev. B **90**, 064503 (2014).
[33] J. Choi, J. Shin, and E. Kim, Phys. Rev. B **92**, 144505 (2015).
[34] X. Mi and J. D. Reppy, J. Low Temp. Phys. **175**, 104 (2013).
[35] I. Iwasa, J. Low Temp. Phys. **171**, 30 (2013).
[36] R. H. Crepeau, O. Heybey, D. Lee, and S. A. Strauss, Phys. Rev. A **3**, 1162 (1971).
[37] D. S. Greywall, Phys. Rev. B **16**, 5127 (1977).
[38] J. Day and J. Beamish, J. Low Temp. Phys. **166**, 33 (2011).
[39] N. Mulders, http://meetings.aps.org/link/BAPS.2012.MAR.A16.7.
[40] S. Sasaki, F. Caupin, and S. Balibar, J. Low Temp. Phys. **153**, 43 (2008).
[41] G. A. Armstrong, A. A. Helmy, and A. S. Greenberg, Phys. Rev. B **20**, 1061 (1979).
[42] D. E. Zmeev and A. I. Golov, Phys. Rev. Lett. **107**, 065302 (2011).
[43] A. F. Schuch and R. L. Mills, Phys. Rev. Lett. **8**, 469 (1962).